LIG1 Is a Synthetic Lethal Target in *BRCA1* Mutant Cancers

Lauren Catherine M. Martires, Leanne G. Ahronian, Charlotte B. Pratt, Nikitha M. Das, Xiaobin Zhang, Douglas A. Whittington, Hongxiang Zhang, Binzhang Shen, Jon Come, Patrick McCarren, Mu-Sen Liu, Chengyin Min, Tianshu Feng, Haris Jahic, Janid A. Ali, Daniel R. Aird, Fang Li, Jannik N. Andersen, Alan Huang, William D. Mallender, and Hilary E. Nicholson

ABSTRACT

Synthetic lethality approaches in *BRCA1/2*-mutated cancers have focused on PARP inhibitors, which are subject to high rates of innate or acquired resistance in patients. In this study, we used CRISPR/Cas9-based screening to identify DNA ligase I (LIG1) as a novel target for synthetic lethality in *BRCA1*-mutated cancers. Publicly available data supported *LIG1* hyperdependence of *BRCA1* mutant cells across a variety of breast and ovarian cancer cell lines. We used CRISPRn, CRISPRi, RNAi, and protein degradation to confirm the lethal effect of *LIG1* inactivation at the DNA, RNA, and protein level in *BRCA1* mutant cells *in vitro*. LIG1 inactivation resulted in viability loss across multiple *BRCA1*-mutated cell lines, whereas no effect was observed in *BRCA1/2* wild-type cell lines, demonstrating target selectivity for the *BRCA1* mutant context. On-target nature of the phenotype was demonstrated through rescue of viability with exogenous wild-type *LIG1* cDNA. Next, we demonstrated a concentration-dependent relationship of LIG1 protein expression and *BRCA1* mutant cell viability using a titratable, degradable LIG1 fusion protein. *BRCA1* mutant viability required LIG1 catalytic activity, as catalytically dead mutant $LIG1^{K568A}$ failed to rescue viability loss caused by endogenous *LIG1* depletion. *LIG1* perturbation produced proportional increases in PAR staining in *BRCA1* mutant cells, indicating a mechanism consistent with the function of LIG1 in sealing ssDNA nicks. Finally, we confirmed *LIG1* hyperdependence *in vivo* using a xenograft model in which LIG1 loss resulted in tumor stasis in all mice. Our cumulative findings demonstrate that LIG1 is a promising synthetic lethal target for development in patients with *BRCA1*-mutant cancers.

Introduction

Inactivation of the *BRCA1* gene is responsible for a large percentage of inherited predispositions to breast and ovarian cancers in women, with associated lifetime risk estimates of 80% and 40% to 65%, respectively (1). Loss or mutation of *BRCA1* has also been associated with colon and prostate cancers in men (2). In December 2014, the FDA approved the first PARP inhibitor for patients with *BRCA1/2*-mutated ovarian cancer, providing clinical proof-of-concept for synthetic lethality as an anticancer strategy. Synthetic lethality describes a gene interaction in which mutation or disruption of one of the interacting genes is compatible with cell viability, but perturbation of both genes produces lethality (3, 4). This concept was first reported in *Drosophila melanogaster* (5) and later articulated in an oncological context by Hartwell and colleagues (6) in the late 1990s. PARP enzymes are involved in base-excision repair of ssDNA breaks as well as nucleotide excision repair and the regulation of end-joining repair of double-strand DNA (dsDNA) breaks (7). In patients with homologous recombination deficiency (HRD), including those with germline *BRCA* (*BRCA1* and/or *BRCA2*) mutations or with nongermline HRD-positive tumors, PARP inhibition is associated with the accumulation of dsDNA breaks and subsequently cell death due to intolerable replication stress at multiple difficult-to-replicate loci (8). Discovery of the synthetic lethal interaction between PARP and BRCA spurred the clinical development of PARP inhibitors as a novel class of anticancer agents and opened new gateways for oncological drug development (9, 10).

To date, several PARP inhibitors have been used successfully as synthetic lethal anticancer agents in the treatment of patients with HRD tumors, specifically, *BRCA1*- and *BRCA2*-mutated ovarian, breast, and pancreatic cancers (11), with ongoing clinical trials in chemoresistant germline or somatic *BRCA1/2*-mutated breast, ovarian, lung, and pancreatic cancers. However, use of these agents, especially for long-term maintenance therapy, is considerably limited by inherent and acquired resistance: approximately half of patients with *BRCA1/2* mutations exhibit pre-existing intrinsic resistance to PARP inhibitors, and more than two-thirds of patients receiving PARP inhibitor therapy eventually develop acquired resistance (12–14). Moreover, the available spectrum of PARP inhibitors is associated with variable tolerability, necessitating dose reduction in some patients (15). Alongside strategies seeking to resensitize patients to treatment, there is a vested interest in identifying other targets with efficacy in *BRCA1/2* mutant cancers that can provide good efficacy and tolerability as stand-alone monotherapy targets, act in concert with PARP inhibitors to improve efficacy, or provide an alternative for patients with intrinsic or acquired resistance to PARP inhibitors.

Molecular target identification for *BRCA1/2*-mutated cancers has been greatly aided by recent advances in CRISPR/Cas9 technology (16). Beyond *PARP1/2*, studies have characterized synthetic lethal interactions of BRCA1/2 with the gene product of *SIRT1/6*, wherein loss of sirtuin activity leads to PARP1/HPF1-mediated serine ADP-ribosylation and loss of viability (17), as well as the gene product of *POLQ*, wherein loss of Polθ activity is selectively lethal in cells deficient for homologous recombination (HR; 18–21). We previously used a CRISPR/Cas9 screen to identify USP1 as a target for synthetic lethality with *BRCA1/2* and demonstrated that perturbation of *USP1*

Tango Therapeutics Inc., Boston, Massachusetts.

Corresponding Author: Hilary E. Nicholson, Tango Therapeutics Inc., 201 Brookline Avenue, Suite 901, Boston, MA 02215. E-mail: hnicholson@tangotx.com

Mol Cancer Ther 2025;XX:XX–XX

doi: 10.1158/1535-7163.MCT-24-0598

in *BRCA1/2* mutant cells is associated with decreased DNA synthesis and accumulation of S phase–specific DNA damage, likely mediated through accumulation and aberrant processing of mono- and poly-ubiquitinated proliferating cell nuclear antigen (PCNA; ref. 22).

In this study, we characterize a second gene hit identified in our CRISPR/Cas9 screen, DNA ligase 1 (*LIG1*), as a target for synthetic lethality in *BRCA1*-mutant cancers. The ATP-dependent DNA ligase LIG1 is encoded by the *LIG1* gene and functions in DNA replication and recombination as well as base excision repair (23), and specifically the processing of Okazaki fragments (24). Our *in vitro* and *in vivo* genetic studies validate LIG1 as a target for oncological development and suggest that synthetic lethality with BRCA1 is dependent on LIG1 catalytic activity, wherein PAR accumulation leads to genomic instability and subsequently cell death.

Materials and Methods

Information for compounds, antibodies, siRNAs, short hairpin RNA (shRNA), and single-guide RNA (sgRNA) sequences, cDNA sequences, and cell lines used in this study are listed in Supplementary Tables S1–S5.

Cloning of sgRNA and cDNA constructs

A lentiviral system was used for both CRISPR-Cas9 and doxycycline inducible CRISPR-dCas9-KRAB cloning. All guide and cDNA sequences are reported in Supplementary Table S4. Wild-type (WT) and mutant cDNA constructs were cloned using gBlocks purchased from Integrated DNA Technologies. dTAG constructs were cloned by using a GS linker to fuse FKBP12 WT or mutant sequences to the C-terminus of the WT LIG1 cDNA sequence. All constructs were verified using Sanger sequencing.

Cell culture and cell line engineering

All *BRCA* mutant and WT cell lines were cultured and maintained at 37°C under 5% CO_2. Cell lines were tested for *Mycoplasma* weekly using the Lonza MycoAlert Detection Kit according to manufacturer's instructions (Lonza Bioscience, LT07-318). Cell line sources and culture media formulations are listed in Supplementary Table S2. Cell lines were authenticated by short tandem repeat performed at Labcorp. All cells were used at or below passage 15 and within 8 weeks of thawing.

For generation of stable cell lines, constructs and lentiviral packaging mix (Cellecta, CPCP-K2A) were transfected into Lenti-X cells using Lipofectamine 3000 (Thermo Fisher Scientific, L3000015). After incubation with transfection reagents overnight, media was replaced with DMEM supplemented with 30% FBS. Media containing viruses was collected 48 hours after transfection and filtered with a 0.45 mm membrane. For infection, cells were incubated overnight in media containing 8 mg/mL polybrene (Sigma-Aldrich) and virus. Infected cells were recovered for 24 hours before selection with puromycin (Gibco, A1113802), blasticidin (Gibco, A1113903), or geneticin (Gibco, 10131035) corresponding to the antibiotic resistance cassette in each plasmid. Where applicable, *LIG1* cDNA expression was titrated to correspond with endogenous levels of LIG1 protein.

For generation of single-cell clones, cells were plated at 2,000 cells/15 cm dish and allowed to grow until single colonies visible. Media was aspirated, and colonies were covered with sterile cloning discs (Thermo Fisher Scientific, 0790710B) soaked in 0.25% trypsin-EDTA and subsequently transferred to a sterile plate containing culture media, allowed to adhere overnight, and cultured as needed for experiments. Successful gene editing was confirmed by Western blotting and Sanger sequencing of genomic DNA (gDNA).

CRISPR-Cas9 screening and manual curation of *BRCA* mutations

The methodology for CRISPR-Cas9 screening and complete findings have been reported previously (25). For corroboration of *LIG1* candidacy in the CRISPR-Cas9 screens, we performed manual curation of *BRCA* mutations in multiple cell lines using publicly available and in-house analyses to evaluate *LIG1* dependence. *BRCA* mutation status was assigned to breast and ovarian cancer cell lines in the Project Achilles database by first aggregating mutation calls from different sources and sequencing technologies [Broad whole-exome sequencing (WES), Sanger WES, CGA WES, and Hybrid capture]. Next, the Ensembl Variant Effect Predictor was used to re-annotate the mutation calls to derive their relative impact scores (high, moderate, etc.). Sample allele counts were aggregated and used to derive the genotype status (zygosity) of each mutation. Loss of function samples had a high impact mutation or a moderate impact, homozygous mutation in *BRCA1*.

Colony formation assays

Engineered cells were seeded onto tissue culture plates at densities such that cells would reach 80% to 90% confluency at endpoint. For doxycycline (DOX)-inducible experiments, cells were seeded with or without 0.5 μg/mL doxycycline; experiments using dTAG-based protein degradation were seeded with the indicated concentration of dTAGv1. Media and treatment were refreshed every 3 to 4 days, and cells were allowed to grow for 14 days. For siRNA experiments, cells were transfected with SMARTpool siRNAs (Horizon Discovery) targeting either a nontargeting control sequence, LIG1 or PLK1 using Lipofectamine 3000 RNAiMAX (Thermo Fisher Scientific 13778100), according to manufacturer's protocol. Cells were incubated with siRNAs overnight and received fresh media the following morning. Cells were re-transfected every 3 to 4 days over a 14-day period. At endpoint, cells were stained with crystal violet, dried, and imaged. For quantification, acetic acid was used to solubilize the dye, and absorbance was measured.

PAR staining and immunofluorescence

Engineered cells were seeded onto 8-well chamber slides (30,000 cells/well) with or without 0.5 μg/mL doxycycline. Cell media and treatment were refreshed on treatment day 2. On day 4, cells were treated with PARGi, fixed in methanol, and subsequently permeabilized and incubated with the antibodies listed in Supplementary Table S2. For each chamber, five fields/image were taken at 20× magnification.

In-cell Western blotting

Engineered cells were seeded onto black-sided, clear-bottom, 96-well tissue culture plates (15,000 cells/well) with or without 0.5 μg/mL doxycycline. The next day, cells were treated with PARGi and methyl methanesulfonate (MMS), fixed in methanol, and subsequently permeabilized and incubated with the antibodies listed in Supplementary Table S2. Fluorescence was visualized using a LI-COR Odyssey imaging system.

Immunoblotting

Protein lysate preparation and immunoblotting were performed, as described previously with minor modifications (25). Antibodies are summarized in Supplementary Table S2. Briefly, cells were rinsed in cold PBS and lysed in EBC buffer supplemented with protease and phosphatase inhibitors and universal nuclease. Lysates were cleared of insoluble material by centrifuging at 20,000 × *g* for 10 minutes at 4°C, and protein concentration was determined with the bicinchoninic acid protein assay.

For traditional Western blotting, 20 to 40 μg of protein in equal volumes was heated in LDS-sample buffer containing dithiothreitol (DTT) for 5 minutes at 95°C. Samples were centrifuged at 20,000 × *g*, separated by SDS-PAGE electrophoresis in 4% to 12% Bis-Tris gels and transferred to nitrocellulose membranes.

For simple Western blotting, 1.8 μg of protein in equal volumes was heated in 0.1× sample buffer containing DTT and fluorescent master mix for Jess (Bio-Techne), loaded onto Jess plates, and processed according to the manufacturer's specifications. For detailed information on all immunoblotting procedures, see the Supplementary Methods.

NAD/NADH assay

NAD+ levels were measured using a NAD/NADH Assay kit (Abcam #ab65348). Assay procedure was performed according to the manufacturer's protocol. MDA-MB-436 cells expressing a DOX-inducible CRISPR-resistant LIG1 cDNA and endogenous LIG1 knockout (KO) were treated with or without 0.5 μg/mL doxycycline for 6 days. Approximately 2 million cells per condition were harvested for NADH/NAD extraction. After removing NAD-consuming enzymes with a 10 kDa spin column (Abcam #ab93349), half of each sample was transferred to new tubes and incubated at 60°C for 30 minutes to decompose NAD+. NADtotal and NAD+ decomposed samples were diluted 1:3 in Extraction Buffer, then incubated with reaction mixture at room temperature for 5 minutes. NADH Developer was added to each well, and the reaction cycled at room temperature for 4 hours. Absorbance was measured at OD 450 nm on a SpectraMax microplate reader (Molecular Devices).

Immunofluorescence staining and assessment of micronuclei

Cells were seeded on #1.5 22 × 22 mm coverslips (Epredia, 152222) in 6-well plates (Corning). After being allowed to adhere for at least 16 hours, cells were washed with PBS and then fixed with 100% methanol (Fisher Chemical, A411-4) for 15 minutes at −20°C. After a PBS wash, 0.5% Triton X-100 (Thermo Fisher Scientific, 85112) in PBS was used to permeabilize cells for 15 minutes at room temperature. After being washed twice with PBS, coverslips were incubated in PBS + 10 μmol/L Hoechst 33342 (Thermo Fisher Scientific, 62249) for 5 minutes at room temperature to stain for DAPI, and then washed with PBS. After drying at room temperature, coverslips were mounted on slides (Thermo Fisher Scientific, 22-178-277) with ProLong Gold Antifade Mountant (Invitrogen, P36930) and allowed to dry for at least 16 hours at room temperature. Cells were imaged via an inverted Zeiss Axio Observer microscope using Zeiss ZEN pro imaging software. Analysis was completed using the cell counter functions of ImageJ software.

Xenograft model in NOG mice

Animal studies were conducted at Pharmaron. Female NOG mice (Vital River) 6 to 8 weeks of age were inoculated subcutaneously on the right flank with p5 MDA-MB-436-pTG59-CloneA or MDA-MB-436-pTG53-CloneD cells (1×10^7 cells per animal) and 50% Matrigel (1:1) in RPMI1640. Doxycycline (25 mg/kg/day, orally) treatment was initiated immediately following implantation. When xenografts had reached a mean volume of ~200 mm^3, animals were randomized into DOX+ (25 mg/kg, every day orally) and DOX− (saline 10 μL/g, every day orally) groups.

Tumor measurements were conducted twice weekly using a caliper and estimated using the formula: tumor volume = $a \times b \times b/2$, where "*a*" and "*b*" are the long and short diameters of the tumor, respectively. Animals were euthanized on day 39 for tissue harvesting and protein quantification. All procedures related to animal handling, care, and treatment were approved by the local Institutional Animal Care and Use Committee and performed in accordance with Association for Assessment and Accreditation of Laboratory Animal Care International guidance.

Statistical analysis

Image quantification was conducted using ImageJ (NIH, Bethesda, MD; RRID: SCR_003070). All statistical analyses were performed using GraphPad Prism (GraphPad, Software Inc.; RRID: SCR_002798).

Data availability

The data generated in this study are available within the article and its Supplementary Materials. Additional information is available on request.

Results

Identification of *LIG1* as a synthetic lethal target in *BRCA1* mutant cell lines

To identify genes, whose inactivation conferred lethality in *BRCA1* mutant, but not WT cells, we conducted CRISPR-Cas9 screens in 13 *BRCA1/2* WT (MDA-MB-231, KP4, HCC1954, HCC70, AU565, A549, HCC38, HGC-27, FADU, 23132/87, SNU638, NUGC-4, and SNU-5) and two *BRCA1* mutant (MDA-MB-436 and SUM149PT) cancer cell lines using a druggable genome library. In addition to the identification of known synthetic lethal targets PARP1 (26), USP1 (22, 27), and Polθ (18), we identified LIG1 as a candidate synthetic lethal target in *BRCA1* mutant cell lines (**Fig. 1A**). Next, we conducted an internal analysis of *BRCA* mutation status for individual breast and ovarian cancer cell lines in the Project Achilles database. *LIG1* lethality scores were tabulated for all included cell lines and confirmed selective hyperdependence of *BRCA1* mutant cell lines on *LIG1* (**Fig. 1B**). To ask whether the dependence on *LIG1* would be extrapolatable to the *BRCA2* mutant context, we analyzed publicly available CRISPR screening data in DepMap (Supplementary Fig. S1A; ref. 28). Cell lines harboring damaging mutations in *BRCA2* were significantly more dependent on *LIG1* as compared with *BRCA2* intact cell lines as demonstrated by more negative Chronos gene effect scores, indicating that mutation in *BRCA1* or *BRCA2* could confer sensitivity to LIG1 inactivation. We also assessed whether a DLD1 cell line pair that is isogenic for *BRCA2* would be differentially sensitive to *LIG1* knockdown based on *BRCA2* status (Supplementary Fig. S1B–S1E). DLD1 cells that were deficient for *BRCA2* were dependent on LIG1 for survival, whereas DLD1 cells with *BRCA2* intact were not impacted by loss of LIG1.

Perturbation of *LIG1* inhibits growth of *BRCA1* mutant cells

To assess the robustness of the synthetic lethal relationship between *LIG1* and *BRCA1*, we used multiple strategies for single-gene perturbation using the MDA-MB-436 cell line, which has a *BRCA1*

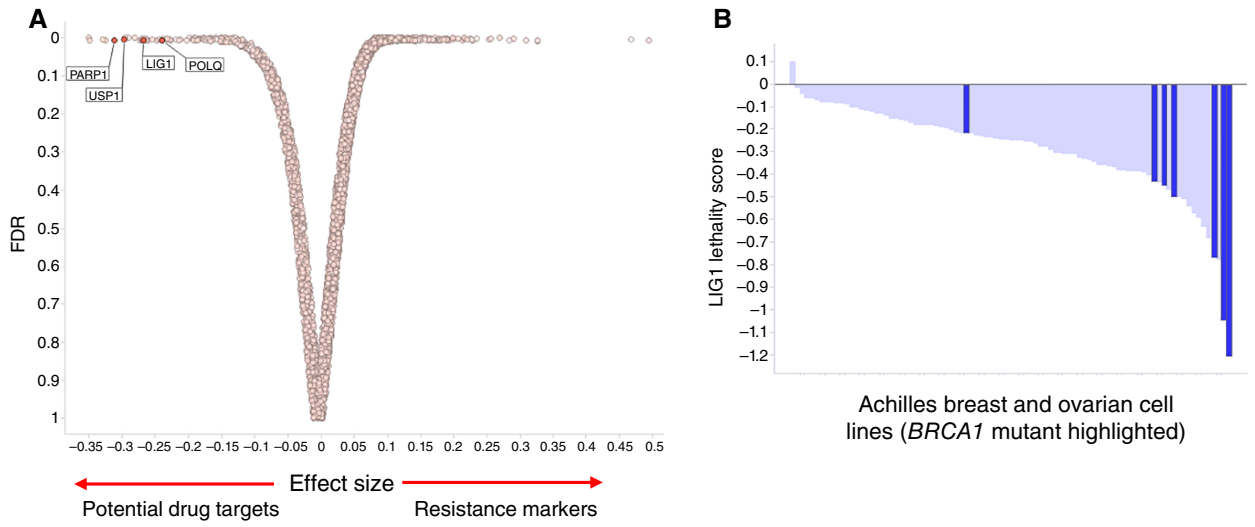

Figure 1.

Hyperdependence of multiple *BRCA1*-mutated cancer cell lines on *LIG1*. **A,** Volcano plot of a MAGeCK analysis comparing CRISPR-Cas9 screens performed in two *BRCA1* mutant and 13 *BRCA1/2* WT breast cancer cell lines (*BRCA1/2* WT: MDA-MB-231, KP4, HCC1954, HCC70, AU565, A549, HCC38, HGC-27, FADU, 23132/87, SNU638, NUGC-4, and SNU-5. *BRCA1* mutant: MDA-MB-436 and SUM149PT.) Genes on the left side of the plot are preferentially depleted in the *BRCA1* mutant cells (potential drug targets), whereas those on the right side are preferentially depleted in *BRCA1/2* WT cells (potential resistance markers) or resulted in enhanced growth of *BRCA1* mutant cells. Known BRCA dependencies (*PARP1*, *USP1*, and *POLQ*) are highlighted. **B,** Waterfall plot of *LIG1* lethality scores for breast and ovarian cancer cell lines. BRCA1 mutations were manually curated for individual cell lines from the Project Achilles database (see "Materials and Methods").

mutation that results in loss of BRCA1 protein expression (29). To assess whether inactivation of *LIG1* at the mRNA level affects growth of *BRCA1* mutant cells, cells were first engineered to express a DOX-inducible CRISPRi guide RNA targeting the promoter of either an intron-targeting control sequence or *LIG1*. Following validation of *LIG1* knockdown by Western blot, a 14-day colony formation assay was performed to assess the impact of *LIG1* knockdown on colony growth (**Fig. 2A**). *LIG1* knockdown reduced colony formation of *BRCA1* mutant cells by 89%. Colony formation of cells expressing the intron-targeting control sequence was unaffected by DOX treatment (Supplementary Fig. S2).

To determine whether perturbation of LIG1 at the protein level affects viability of *BRCA1* mutant cells, we engineered MDA-MB-436 cells to express a CRISPR-resistant *LIG1* cDNA (crLIG1) fused to either the FKBP12wt degron (nondegradable) or FKBP12mut (dTAG) degron (degradable) to produce a titratable degradable LIG1 protein [for dTAG model details, see (30)]. Viral titer and promoter strength were selected to approximate levels of endogenous LIG1 protein expression. These cells were then edited to knock out endogenous *LIG1*. Treatment with increasing concentrations of the degron-mediated PROTAC dTAGv1 produced concentration-dependent loss of LIG1-dTAG protein as well as concentration-dependent decreases in colony formation (**Fig. 2B**; Supplementary Fig. S3), whereas no effect was observed in cells expressing the nondegradable LIG1 cDNA (crLIG1-FKBP12wt). These findings support the hyperdependence of the *BRCA1* mutant cell line MDA-MB-436 on LIG1 expression.

LIG1 synthetic lethality is on-target and selective for *BRCA1* mutant lines

To ask whether the LIG1 dependence discovered in our screen was on-target and specific for the *BRCA1* mutant context, we engineered the *BRCA1* mutant cell line MDA-MB-436 and the *BRCA1/2* WT HCC1954 cell line to express a DOX-inducible CRISPR-resistant *LIG1* cDNA and edited the endogenous *LIG1* gene to produce complete KO of endogenous *LIG1*. In this model, withdrawal of DOX results in complete depletion of all *LIG1* (and thus loss of LIG1 protein). DOX withdrawal reduced colony formation in *BRCA1* mutant cells by 87% but had no effect on colony formation of *BRCA1/2* WT cells (**Fig. 3A** and **B**). These data demonstrate that the loss of viability in *BRCA1* mutant cells is on-target through *LIG1* as the inducible *LIG1* cDNA fully rescued the effect of endogenous *LIG1* KO, and that the dependence on *LIG1* is specific to the *BRCA1* mutant context. These results were recapitulated using MDA-MB-436 cells engineered to be isogenic through re-expression of *BRCA1*. Using this isogenic pair, knockdown of *LIG1* eliminates colony formation in *BRCA1* mutant MDA-MB-436 cells expressing an empty vector control plasmid, whereas re-expression of *BRCA1* rescues this viability defect despite similar level of *LIG1* depletion (Supplementary Fig. S4).

To investigate whether our findings in MDA-MB-436 and HCC1954 cell lines were representative of responses in a wider range of *BRCA1* mutant and *BRCA* WT cell lines, we engineered DOX-inducible shRNAs targeting *LIG1*, *PLK1* (pan-lethal control), or a control sequence in five *BRCA1* mutant cell lines (MDA-MB-436, COV362, SUM149PT, HCC1395, and UWB1.289) and three *BRCA1/2* WT cell lines (HCC1954, HCC1419, and AU565). *LIG1* knockdown selectively reduced viability in *BRCA1* mutant cell lines but not *BRCA1/2* WT cell lines (**Fig. 3C** and **D**). These data demonstrate that the synthetic lethality between *LIG1* and *BRCA1* is true across a variety of cell lines, indicating the robustness of the relationship. Furthermore, we asked whether the homologous recombination deficient (HRD+) but BRCA1/2 WT cell line HCC1806 (31) was dependent on LIG1 for survival. *LIG1* knockdown

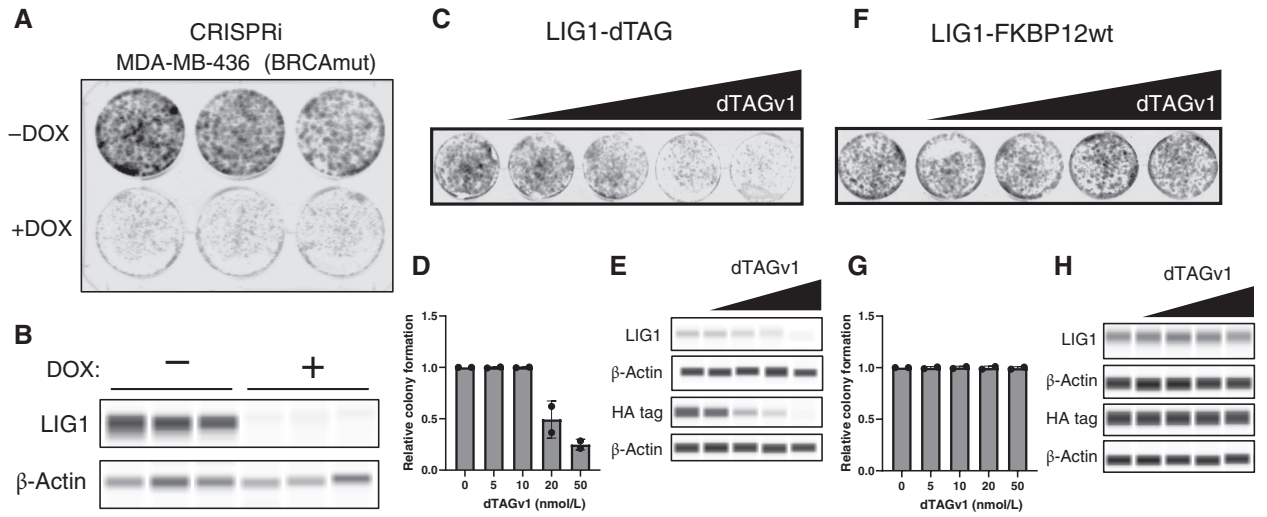

Figure 2.

Perturbation of *LIG1* is lethal in *BRCA1*-mutated cancer cells. Colony formation assays (treatment day 14) in MDA-MB-436 cells engineered to express (**A** and **B**) a DOX-inducible CRISPRi guide RNA targeting either an intron-targeting control sequence (Supplementary Fig. S2) or the promoter of *LIG1*, or a CRISPR-resistant *LIG1* cDNA fused to either the FKBP12mut (dTAG) degron (degradable; **C–E**) or the FKBP12wt degron (nondegradable; **F–H**), with KO of endogenous *LIG1*. **B, E,** and **H,** Model validation with Western blotting on treatment day 4 (quantified in Supplementary Fig. S3). **E** and **G,** Corresponding quantifications of relative viability on treatment day 14 ($N = 2$ biological replicates).

inhibited colony formation in this cell line (Supplementary Fig. S5), indicating that LIG1 dependence may be a feature of HRD beyond *BRCA1* inactivation.

Catalytic activity of LIG1 is required for *BRCA1* mutant cell viability

We next asked whether the catalytic activity of LIG1 is necessary for *BRCA1* mutant cell viability. To perform its enzymatic function of sealing single-stranded nicks in the DNA backbone, the LIG1 protein transfers an AMP molecule onto the DNA nick. Lys568 is critical for the catalytic activity of LIG1 due to its role in hydrolyzing ATP and coordinating the AMP moiety, and the K568A mutant produces a catalytically inactive form of the enzyme (**Fig. 4A**; refs. 32, 33). *BRCA1* mutant MDA-MB-436 cells were engineered to express a shRNA-resistant WT or $LIG1^{K568A}$ mutant cDNA alongside a DOX-inducible shRNA targeting *LIG1*. Consistent with previous observations, *LIG1* knockdown reduced growth of MDA-MB-436 cells (no cDNA) in 14-day colony formation assays. This loss of viability was rescued by expression of an shRNA-resistant WT *LIG1* cDNA. In contrast, expression of the catalytically dead $LIG1^{K568A}$ mutant was not sufficient to rescue the loss of viability resultant from endogenous *LIG1* depletion (**Fig. 4B** and **C**). These findings indicate that the catalytic activity of LIG1 is required for survival of *BRCA1* mutant cells.

LIG1 inactivation leads to increased PARylation and chromosomal instability

LIG1 suppresses ssDNA gaps and DNA nicks through its activity ligating Okazaki fragments and through its role in DNA damage repair. In the absence of ligation, unligated DNA nicks are subject to PARylation to signal for the recruitment of DNA repair machinery (34, 35). We examined the effect of functional LIG1 expression on PARylation to further elucidate the mechanism of *LIG1* synthetic lethality with *BRCA1*. Cells expressing an shRNA-resistant WT or $LIG1^{K568A}$ mutant cDNA alongside a DOX-inducible shRNA targeting *LIG1* were subject to immunofluorescence (IF)-based staining for PAR. Knockdown of *LIG1* led to a ~19× increase in PAR staining, and this effect could be completely rescued by expression of the shRNA-resistant *LIG1*. In contrast, expression of the catalytically inactive $LIG1^{K568A}$ mutant was not sufficient to rescue induction of PAR caused by endogenous *LIG1* knockdown (**Fig. 5A** and **B**). To corroborate the PAR signal observed with *LIG1* mRNA knockdown, we engineered to express DOX-inducible *LIG1* cDNA with endogenous *LIG1* gene KO to ask whether the same phenomenon could be observed when inactivating *LIG1* at the DNA level. Consistent with our shRNA knockdown results, DOX withdrawal (and thus loss of *LIG1* expression) led to an increase in PARylation as measured by in-cell Western blotting (Supplementary Fig. S6). These data demonstrate that loss of functional LIG1 expression is associated with increased PARylation in *BRCA1* mutant cells, consistent with its role in sealing DNA nicks.

We next asked whether there was a concentration-dependent relationship between the level of LIG1 protein and accumulation of PARylation using titratable degradation of LIG1 fusion proteins (LIG1-dTAG or LIG1-FKBP12wt control) in cells with endogenous *LIG1* KO. Increasing concentrations of dTAGv1 resulted in concentration-dependent loss of LIG1-dTAG protein as well as concentration-dependent increases in the ratio of PAR/DRAQ5 IF, whereas no effect was observed in cells expressing the nondegradable LIG1 fusion protein (LIG1-FKBP12wt; **Fig. 5C**). Findings support the hypothesis that loss of LIG1 activity is directly responsible for associated increases in PARylation observed in *BRCA1* mutant cells, and that this effect is proportional to the amount of LIG1 protein available to seal DNA nicks. PARP1 uses the cofactor NAD+ to add PAR chains to unligated DNA nicks. Consistent with this requirement, we observed a significant decrease in NAD+ level in cells lacking *LIG1* in a model where endogenous *LIG1* has been knocked out using CRISPR (sgLIG1) and an exogenous Dox-inducible *LIG1* cDNA had been stably expressed (Supplementary Fig. S5C).

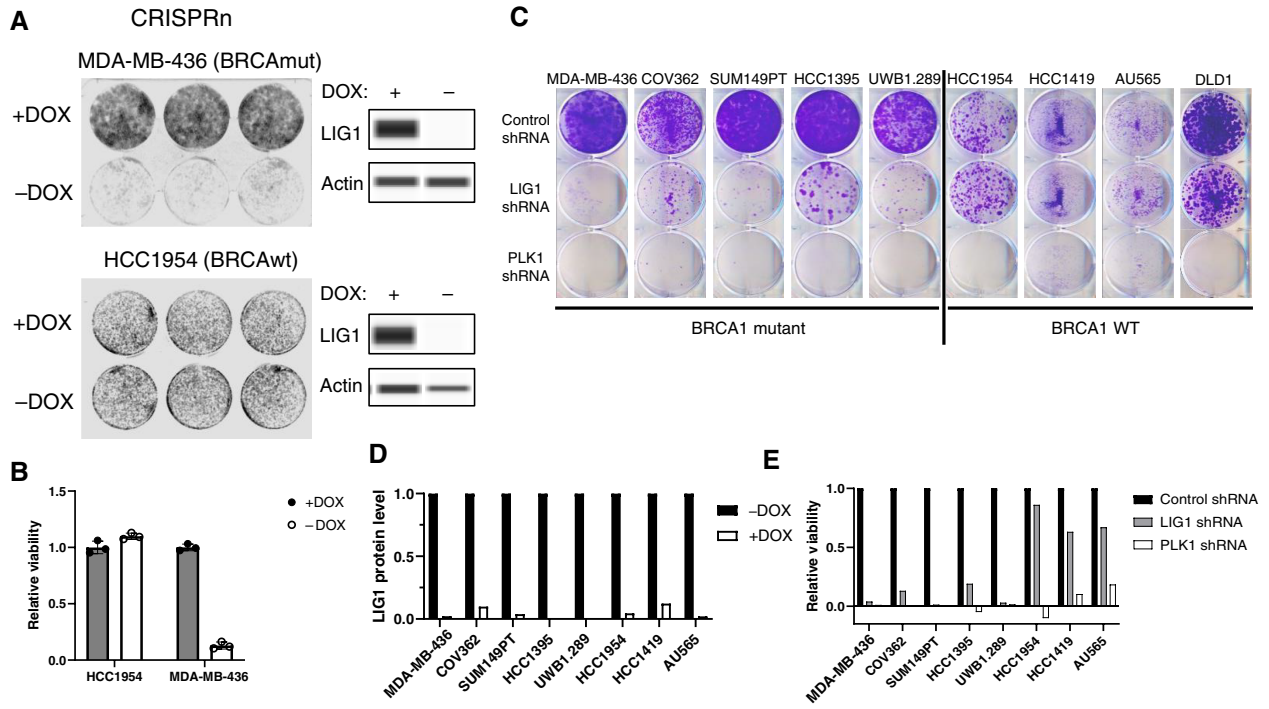

Figure 3.

LIG1 is a selective synthetic lethal target in *BRCA1*-mutated cell lines. Representative image (**A**) and quantification (**B**) of colony formation assay (treatment day 14) in MDA-MB-436 (*BRCA1* mutant) and HCC1954 (*BRCA* WT) cells engineered to express a DOX-inducible CRISPR-resistant *LIG1* cDNA with KO of endogenous *LIG1*. Right, model validation with Western blotting on treatment day 4. Representative colony formation assay (treatment day 14; **C**) and quantification (**E**) in five *BRCA1* mutant cell lines (MDA-MB-436, COV362, SUM149PT, HCC1395, and UWB1.289) and three *BRCA1/2* WT cell lines (HCC1954, HCC1419, and AU565) using DOX-inducible shRNA against *LIG1*, *PLK1* (pan-lethal control), or a control sequence. **D,** Model validation with quantification of Western blots on treatment day 4.

No significant change in NAD+ level was observed in cells expressing an sgRNA targeting an intron and expressing exogenous Dox-inducible *LIG1* cDNA.

The increase in PARylation observed when *LIG1* is inactivated is consistent with our hypothesized mechanism in which loss of LIG1 activity leads to accumulation of unligated DNA and genomic

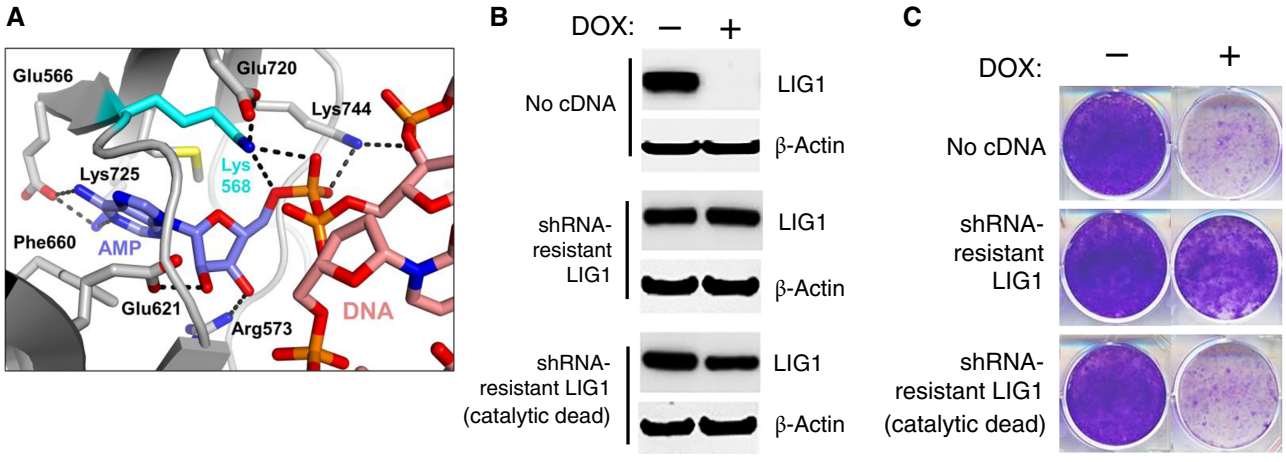

Figure 4.

Catalytic activity of LIG1 is required for viability in *BRCA1*-mutated cells. **A,** Illustrated crystal structure (PDB 6P0A) of LIG1 with nicked dsDNA. Lys568 is shown in cyan blue, AMP is shown in purple, and DNA is shown in coral. The K568A mutation produces a catalytically inactive LIG1 protein. **B,** Model validation with Western blotting on treatment day 4. **C,** Colony formation assay (treatment day 14) in MDA-MB-436 cells engineered to express an shRNA-resistant WT or *LIG1*^{K568A} mutant cDNA alongside a DOX-inducible shRNA targeting *LIG1*.

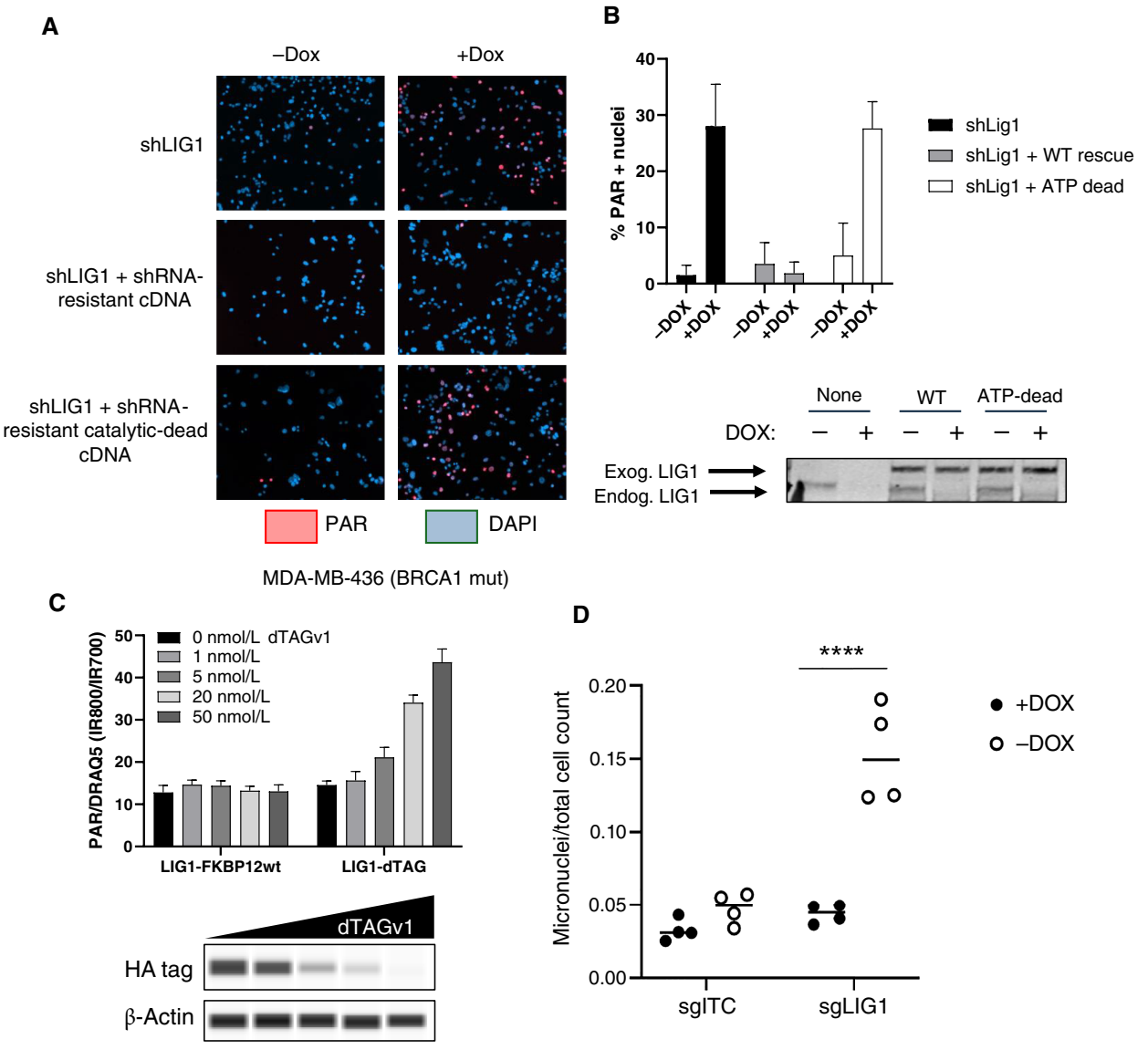

Figure 5.

Perturbation of LIG1 induces PAR accumulation and micronuclei formation in *BRCA1*-mutated cells. **A** and **B,** Representative image (**A**) and quantification (**B**, top) of PAR IF on treatment day 4 in MDA-MB-436 cells expressing an shRNA-resistant WT or *LIG1*^{K568A} mutant cDNA alongside a DOX-inducible shRNA targeting *LIG1*. **B,** Bottom, model validation with Western blotting on treatment day 3. **C,** Top, quantification of PAR/DRAQ5 (800 nm/700 nm) IF ratio on treatment day 4 in a model of titratable degradation of LIG1, using MDA-MB-436 cells engineered to express LIG1-dTAG (or LIG1-FKBP12wt control) fusion proteins with endogenous *LIG1* KO. Bottom, model validation with Western blotting. **D,** Quantification of micronuclei relative to total cell count measured by IF staining (one-way ANOVA $P < 0.0001$, Tukey multiple comparisons test sgLIG1 +DOX vs. −DOX $P < 0.0001$) in MDA-MB-436 cells expressing Dox-inducible *LIG1* cDNA and either endogenous *LIG1* KO (sgLIG1) or an intron-targeting control sgRNA (sgITC). ****, $P < 0.0001$ Endog., endogenous; Exog., exogenous.

instability. To assess this, we measured the number of micronuclei in cells with or without *LIG1* knockdown using IF and normalized to total cell number (**Fig. 5D**). We observed a significant increase in the number of micronuclei in cells with *LIG1* knockdown as compared with cells harboring shRNA targeting a control sequence. The formation of micronuclei is consistent with genomic instability as a mechanism leading to cell death.

Loss of *LIG1* inhibits tumor growth *in vivo*

A murine xenograft model was used to ask whether the results of our *in vitro* studies could translate to an *in vivo* setting. MDA-MB-436 cells engineered to express a DOX-inducible CRISPR-resistant *LIG1* cDNA in the presence (sgLIG1) or absence (sgITC) of endogenous *LIG1* KO were xenografted into NOG mice, and tumors were allowed to form under DOX treatment (25 mg/kg/day, orally). Once tumors were established, mice were randomized into two groups, and DOX treatment was maintained (+DOX) or withdrawn (−DOX) to sustain or remove LIG1 expression, respectively. Whereas DOX treatment had no influence on tumor volume in sgITC clone tumors expressing endogenous *LIG1* [**Fig. 6A**; 2,602 mm^3 vs. 2,326 mm^3, T/C value = 88%, P = not significant

(N.S.)], withdrawal of DOX (and subsequent loss of exogenous *LIG1* expression) was associated with significant tumor growth inhibition in tumors lacking endogenous *LIG1* (**Fig. 6B**; 2019 mm^3 vs. 351 mm^3, T/C value = 8%, $P < 0.0001$). Loss of LIG1 expression was confirmed by Western blotting in sgLIG1-DOX mice at an early time point (day 3; **Fig. 6C**) to confirm the model and at endpoint (day 29; Supplementary Fig. S7). Consistent with our observations, *in vitro*, loss of LIG1 suppressed *BRCA1* mutant tumor growth *in vivo*.

Discussion

In this study, we demonstrate synthetic lethality between *LIG1* and *BRCA1* using *in vitro* and *in vivo* genetic strategies. Perturbation of *LIG1* resulted in on-target loss of viability in *BRCA1* mutant cells across multiple cell lines and exhibited selectivity for *BRCA1* mutant cells by lacking this effect in cell lines expressing functional *BRCA1*. This hyperdependence of *BRCA1* mutant cells on *LIG1* was corroborated by consistent results whether perturbing *LIG1* at the DNA, mRNA, or protein level. Although the greatest depth of inquiry relies on MDA-MB-436 cells, our cell line panel in **Fig. 3C** indicates that the results are robust and likely generalizable for the BRCA mutant context. The growth inhibition induced by *LIG1* inactivation could be completely rescued by reconstitution of exogenous *LIG1*, demonstrating the on-target nature of the effect but could not be rescued by supplementation of a catalytically inactive LIG1. Loss of LIG1 catalytic activity was associated with increased PARylation, formation of micronuclei, and inhibition of cell growth, consistent with the known role of LIG1 in DNA replication and damage repair. *LIG1* was also necessary for *BRCA1* mutant tumor growth in a murine xenograft model. Taken together, these data demonstrate that *LIG1* is a validated target for synthetic lethality in *BRCA1*-associated cancers. The identification and development of novel stand-alone targets such as LIG1 for treating *BRCA1* mutant cancers is important for potential future clinical practice in both initial and long-term maintenance treatment of patients harboring *BRCA1* mutant tumors.

Clinically, PARP inhibitors are an important therapeutic option for patients with *BRCA1*-mutated cancers. However, the clinical utility of these agents is limited by inherent or acquired resistance (12–14), highlighting the need for alternative targets. Inhibitors of ideal targets should capably substitute for PARP inhibitors where necessary, facilitate resensitization, or act synergistically in combination therapy with PARP inhibitors or other anticancer agents. Recently, several new targets for synthetic lethality with *BRCA1/2* have been proposed or identified in the literature and share a common mechanism in which loss of a compensatory DNA repair pathway leads to genomic instability (36). BRCA proteins play important roles in several steps of the DNA damage response, including cell-cycle checkpoint activation and repair of dsDNA breaks through HR (37, 38). Accordingly, synthetic lethality targets frequently interact with BRCA either directly or indirectly in processes that maintain genome integrity. Patel and colleagues (36) recently summarized such synthetic lethal interactions for BRCA1/2 and the gene products of *PARP*, *POLQ*, *RAD52*, *FANCD2*, *FEN1*, and *APEX2*. Common to many of these *BRCA1/2* synthetic lethal targets is the generation of single-strand gaps or double-strand breaks (DSB) that result from their loss. Recent studies indicate that

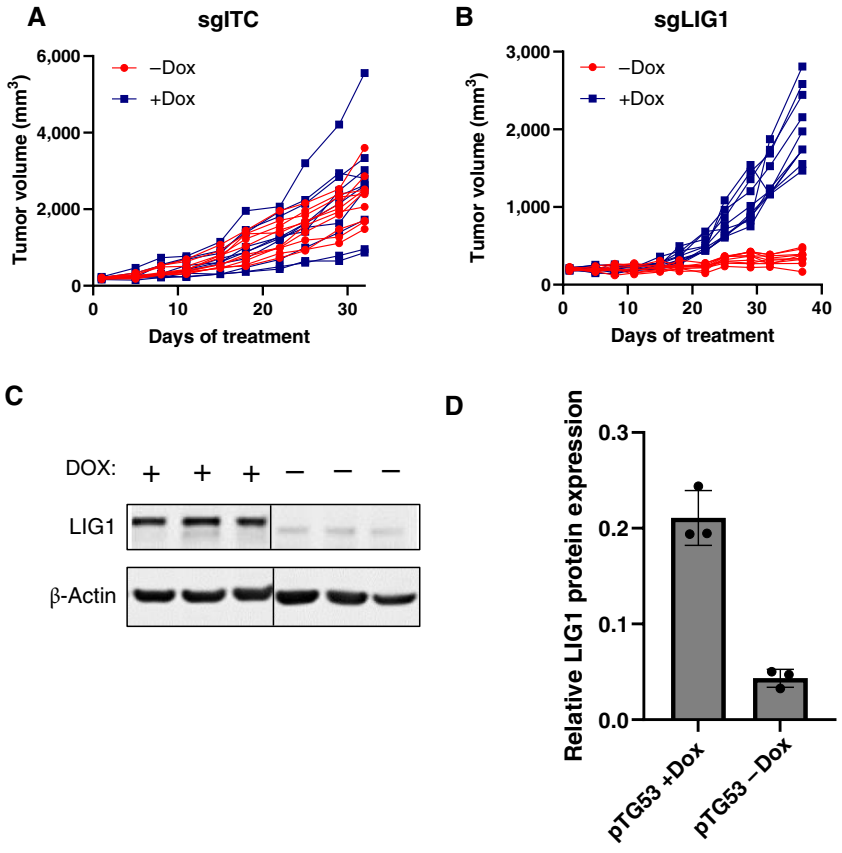

Figure 6.

LIG1 inactivation inhibits *BRCA1* mutant tumor growth in a murine xenograft model. **A** and **B,** Immunodeficient mice were grafted with MDA-MB-436 cells engineered to express a DOX-inducible CRISPR-resistant *LIG1* cDNA in the presence (sgLIG1, **A**) or absence (sgITC, **B**) of endogenous *LIG1* KO. Following tumor establishment under DOX treatment, DOX treatment was maintained (+DOX) or withdrawn (−DOX) to sustain or remove LIG1 expression, respectively. Mice grafted with sgLIG1 and sgITC clones were euthanized on treatment days 37 and 32, respectively. Representative image (**C**) and quantification (**D**) of model validation with Western blotting on treatment day 3.

unresolved ssDNA gaps lead to synthetic lethality with *BRCA1* (39–41), whereas an alternative hypothesis proposes that single-stranded gaps become DSBs, which then depend on HR for repair. Inactivation of *LIG1* could contribute to both proposed mechanisms, through formation of ssDNA by failure to seal nicked DNA at Okazaki fragments due to the role of LIG1 in normal DNA replication or by virtue of loss of the backup DSB repair through the role of LIG1 in alternative end joining (42).

The present research identifies LIG1, the gene product of *LIG1*, as a stand-alone oncological target that is synthetic lethal with *BRCA1* inactivation. LIG1 functions in DNA replication and recombination as well as base excision repair (26); specifically, LIG1 ligates Okazaki fragments and participates in nucleotide resection and DNA repair processes through interaction with PCNA (27) or through interaction with DNA polymerases. In addition to a clear avenue for synthetic lethality with *BRCA1*, these critical roles for LIG1 have also led to its implication as a target for oncological treatment development or as a prognostic biomarker in other cancer settings. Ali and colleagues (43) recently reported synthetic lethality of *LIG1* in *XRCC1*-deficient cancers, and further demonstrated that LIG1 overexpression predicts platinum resistance in this subset. Overexpression of LIG1 has also been identified in several human breast cancers (44, 45). Loss of LIG1 activity has been proposed to mediate anticancer effects by blocking replication, by introducing mutations due to DNA repair pathway failures, and by sensitizing cells to DNA-damaging chemotherapeutic agents (43). To this end, LIG1 is a therapeutic target with wide potential applications in oncology, including its utility as a target for monotherapy in *BRCA1*-mutant cancers.

In previous research, we demonstrated synthetic lethality between *USP1* and *BRCA1/2* via a mechanism involving reduction in the level of PCNA, which acts as a sliding clamp for DNA replication machinery and furthermore illustrated synergy with PARP inhibition (22). Although our data demonstrate the potential for LIG1 as a stand-alone target in *BRCA1*-mutant cancers, it may be hypothesized that LIG1 inhibition has potential to exhibit synergy with PARP inhibitors in the same manner. Consistent with our observations in the present study, Hanzlikova and colleagues (34) demonstrated that perturbation of *LIG1* increases S-phase PARylation due to an accumulation of unligated Okazaki fragments and subsequent PARP activity. Following *LIG1* inactivation, PARylation led to the recruitment of XRCC1, indicating that PARP activity recruits the single-strand break repair pathway as "backup" to process unligated Okazaki fragments. Therefore, simultaneous inhibition of LIG1 and PARP in *BRCA1* mutant cells may produce synergistic lethality, a possibility that merits future investigation in the interest of expanding the efficacy and utility of current PARP inhibitors. While many mechanisms for intrinsic and acquired resistance to PARP inhibitors have been proposed (46, 47), our data using *BRCA1* re-expression to rescue *LIG1* knockdown-induced growth inhibition in MDA-MB-436 cells (Supplementary Fig. S4) suggest that PARP inhibitor resistance caused by restoration of homologous repair capability would not likely present a context that would respond to *LIG1* inactivation. Additional mechanisms with homologous recombination deficiencies (HRD+) may be dependent on LIG1, as demonstrated by the sensitivity to *LIG1* knockdown observed in HRD+, BRCA1/2 WT HCC1806 cells (Supplementary Fig. S5).

In conclusion, the findings of this study identify and validate LIG1 as a promising target for synthetic lethality in *BRCA1*-mutant cancers. In cells with mutated *BRCA1*, loss of functional LIG1 expression reduces growth of *BRCA1*-mutant cancer cells and is associated with increased PARylation. LIG1 inhibition is thus an attractive option for complementing the current arsenal of anticancer agents for the treatment of patients with gynecological and other cancers.

Authors' Disclosures

L.C.M. Martires, L.G. Ahronian, C.B. Pratt, N.M. Das, X. Zhang, D.A. Whittington, H. Zhang, B. Shen, J. Come, P. McCarren, M.-S. Liu, C. Min, T. Feng, H. Jahic, J.A. Ali, D.R. Aird, F. Li, J.N. Andersen, A. Huang, W.D. Mallender, and H.E. Nicholson report other support from Tango Therapeutics outside the submitted work.

Authors' Contributions

L.C.M. Martires: Data curation, formal analysis, validation, investigation, visualization, methodology, writing–original draft, writing–review and editing. **L.G. Ahronian:** Conceptualization, validation, investigation, visualization, methodology. **C.B. Pratt:** Validation, investigation, methodology. **N.M. Das:** Validation, investigation, methodology. **X. Zhang:** Validation, investigation, methodology. **D.A. Whittington:** Conceptualization, data curation, writing–review and editing. **H. Zhang:** Conceptualization, validation, investigation. **B. Shen:** Resources, investigation. **J. Come:** Supervision, writing–review and editing. **P. McCarren:** Supervision, visualization, writing–review and editing. **M.-S. Liu:** Investigation, writing–review and editing. **C. Min:** Conceptualization, investigation. **T. Feng:** Investigation. **H. Jahic:** Validation, investigation. **J.A. Ali:** Conceptualization, supervision. **D.R. Aird:** Investigation. **F. Li:** Data curation, software. **J.N. Andersen:** Conceptualization, supervision, writing–review and editing. **A. Huang:** Conceptualization, supervision. **W.D. Mallender:** Conceptualization, supervision, project administration, writing–review and editing. **H.E. Nicholson:** Conceptualization, data curation, formal analysis, supervision, validation, investigation, visualization, methodology, writing–original draft, writing–review and editing.

Acknowledgments

The authors thank their partners at Pharmaron Inc (Beijing, China) for their support of our *in vivo* pharmacology studies, particularly Tan Pang, Yingying Ma, Pengwei Pan, and Dong Qiao. They also thank Katherine Lazarides and Madhavi Bandi for guidance in development of PAR in-cell Western assay. They thank Yi Yu and his team for computational biology support and Antoine Simoneau for his technical advice for mechanism of action studies. The studies in this body of work were funded by Tango Therapeutics.

Note

Supplementary data for this article are available at Molecular Cancer Therapeutics Online (http://mct.aacrjournals.org/).

Received July 19, 2024; revised November 8, 2024; accepted January 22, 2025; published first January 25, 2025.

References

1. Kuchenbaecker KB, Hopper JL, Barnes DR, Phillips K-A, Mooij TM, Roos-Blom M-J, et al. Risks of breast, ovarian, and contralateral breast cancer for BRCA1 and BRCA2 mutation carriers. JAMA 2017;317:2402–16.
2. Ford D, Easton DF, Bishop DT, Narod SA, Goldgar DE. Risks of cancer in BRCA1-mutation carriers. Breast Cancer Linkage Consortium. Lancet 1994;343:692–5.
3. Bortlíková L, Müller P, Vojtěšek B, Rak V, Svoboda M. Synthetic lethality - its current application and potential in oncological treatment. Klin Onkol 2019; 32(Suppl 3):19–24.
4. Kaelin WG Jr. The concept of synthetic lethality in the context of anticancer therapy. Nat Rev Cancer 2005;5:689–98.

5. Dobzhansky T. Genetics of natural populations; recombination and variability in populations of Drosophila pseudoobscura. Genetics 1946;31:269–90.
6. Hartwell LH, Szankasi P, Roberts CJ, Murray AW, Friend SH. Integrating genetic approaches into the discovery of anticancer drugs. Science 1997;278: 1064–8.
7. Murthy P, Muggia F. PARP inhibitors: clinical development, emerging differences, and the current therapeutic issues. Cancer Drug Resist 2019;2: 665–79.
8. Ragupathi A, Singh M, Perez AM, Zhang D. Targeting the BRCA1/2 deficient cancer with PARP inhibitors: clinical outcomes and mechanistic insights. Front Cell Dev Biol 2023;11:1133472.
9. Lord CJ, Ashworth A. PARP inhibitors: synthetic lethality in the clinic. Science 2017;355:1152–8.
10. Lord CJ, Tutt ANJ, Ashworth A. Synthetic lethality and cancer therapy: lessons learned from the development of PARP inhibitors. Annu Rev Med 2015;66: 455–70.
11. O'Malley DM, Krivak TC, Kabil N, Munley J, Moore KN. PARP inhibitors in ovarian cancer: a review. Target Oncol 2023;18:471–503.
12. Dilmac S, Ozpolat B. Mechanisms of PARP-inhibitor-resistance in BRCA-mutated breast cancer and new therapeutic approaches. Cancers (Basel) 2023; 15:3642.
13. Liu FW, Tewari KS. New targeted agents in gynecologic cancers: synthetic lethality, homologous recombination deficiency, and PARP inhibitors. Curr Treat Options Oncol 2016;17:12.
14. Pilié PG, Gay CM, Byers LA, O'Connor MJ, Yap TA. PARP inhibitors: extending benefit beyond BRCA-mutant cancers. Clin Cancer Res 2019;25: 3759–71.
15. Cai Z, Liu C, Chang C, Shen C, Yin Y, Yin X, et al. Comparative safety and tolerability of approved PARP inhibitors in cancer: a systematic review and network meta-analysis. Pharmacol Res 2021;172:105808.
16. Huang A, Garraway LA, Ashworth A, Weber B. Synthetic lethality as an engine for cancer drug target discovery. Nat Rev Drug Discov 2020;19:23–38.
17. Bajrami I, Walker C, Krastev DB, Weekes D, Song F, Wicks AJ, et al. Sirtuin inhibition is synthetic lethal with BRCA1 or BRCA2 deficiency. Commun Biol 2021;4:1270.
18. Ronson GE, Starowicz K, Anthony EJ, Piberger AL, Clarke LC, Garvin AJ, et al. Mechanisms of synthetic lethality between BRCA1/2 and 53BP1 deficiencies and DNA polymerase theta targeting. Nat Commun 2023; 14:7834.
19. Belan O, Sebald M, Adamowicz M, Anand R, Vancevska A, Neves J, et al. POLQ seals post-replicative ssDNA gaps to maintain genome stability in BRCA-deficient cancer cells. Mol Cell 2022;82:4664–80.e9.
20. Higgins GS, Boulton SJ. Beyond PARP-POLθ as an anticancer target. Science 2018;359:1217–8.
21. Ceccaldi R, Liu JC, Amunugama R, Hajdu I, Primack B, Petalcorin MIR, et al. Homologous-recombination-deficient tumours are dependent on Polθ-mediated repair. Nature 2015;518:258–62.
22. Simoneau A, Engel JL, Bandi M, Lazarides K, Liu S, Meier SR, et al. Ubiquitinated PCNA drives USP1 synthetic lethality in cancer. Mol Cancer Ther 2023;22:215–26.
23. Maffucci P, Chavez J, Jurkiw TJ, O'Brien PJ, Abbott JK, Reynolds PR, et al. Biallelic mutations in DNA ligase 1 underlie a spectrum of immune deficiencies. J Clin Invest 2018;128:5489–504.
24. Blair K, Tehseen M, Raducanu V-S, Shahid T, Lancey C, Rashid F, et al. Mechanism of human Lig1 regulation by PCNA in Okazaki fragment sealing. Nat Commun 2022;13:7833.
25. Shields JA, Meier SR, Bandi M, Mulkearns-Hubert EE, Hajdari N, Ferdinez MD, et al. VRK1 is a synthetic-lethal target in VRK2-deficient glioblastoma. Cancer Res 2022;82:4044–57.
26. Farmer H, McCabe N, Lord CJ, Tutt ANJ, Johnson DA, Richardson TB, et al. Targeting the DNA repair defect in BRCA mutant cells as a therapeutic strategy. Nature 2005;434:917–21.
27. Lim KS, Li H, Roberts EA, Gaudiano EF, Clairmont C, Sambel LA, et al. USP1 is required for replication fork protection in BRCA1-deficient tumors. Mol Cell 2018;72:925–41.e4.
28. Broad DepMap. DepMap 24Q2 public. Figshare+. Dataset; 2024. 10.25452/figshare.plus.25880521.v1.
29. Elstrodt F, Hollestelle A, Nagel JH, Gorin M, Wasielewski M, van den Ouweland A, et al. BRCA1 mutation analysis of 41 human breast cancer cell lines reveals three new deleterious mutants. Cancer Res 2006;66:41–5.
30. Nabet B, Roberts JM, Buckley DL, Paulk J, Dastjerdi S, Yang A, et al. The dTAG system for immediate and target-specific protein degradation. Nat Chem Biol 2018;14:431–41.
31. Ma J, Shah R, Bell AC, McDermott N, Pei X, Selenica P, et al. Increased synthetic cytotoxicity of combinatorial chemoradiation therapy in homologous recombination tumors. Int J Radiat Oncol Biol Phys 2024 Jul 10 [Epub ahead of print].
32. Luo J, Barany F. Identification of essential residues in Thermus thermophilus DNA ligase. Nucleic Acids Res 1996;24:3079–85.
33. Sriskanda V, Schwer B, Ho CK, Shuman S. Mutational analysis of Escherichia coli DNA ligase identifies amino acids required for nick-ligation in vitro and for in vivo complementation of the growth of yeast cells deleted for CDC9 and LIG4. Nucleic Acids Res 1999;27:3953–63.
34. Hanzlikova H, Kalasova I, Demin AA, Pennicott LE, Cihlarova Z, Caldecott KW. The importance of poly(ADP-ribose) polymerase as a sensor of unligated Okazaki fragments during DNA replication. Mol Cell 2018;71:319–31.e3.
35. van Wietmarschen N, Nussenzweig A. Mechanism for synthetic lethality in BRCA-deficient cancers: no longer lagging behind. Mol Cell 2018;71:877–8.
36. Patel PS, Algouneh A, Hakem R. Exploiting synthetic lethality to target BRCA1/2-deficient tumors: where we stand. Oncogene 2021;40:3001–14.
37. Fu X, Tan W, Song Q, Pei H, Li J. BRCA1 and breast cancer: molecular mechanisms and therapeutic strategies. Front Cell Dev Biol 2022;10:813457.
38. Roy R, Chun J, Powell SN. BRCA1 and BRCA2: different roles in a common pathway of genome protection. Nat Rev Cancer 2011;12:68–78.
39. Cong K, Peng M, Nedergaard Koushold A, Lee WTC, Lee S, Naya S, et al. Replication gaps are a key determinant of PARP inhibitor synthetic lethality with BRCA deficiency. Mol Cell 2021;81:3128–44.e7.
40. da Costa AA, Somuncu O, Ravindranathan R, Mukkavalli S, Martignetti DB, Nguyen H, et al. Single-stranded DNA gap accumulation is a functional biomarker for USP1 inhibitor sensitivity. Cancer Res 2024;84:3435–46.
41. Panzarino NJ, Krais JJ, Cong K, Peng M, Mosqueda M, Nayak SU, et al. Replication gaps underlie BRCA-deficiency and therapy response. Cancer Res 2021;81:1388–97.
42. Lu G, Duan J, Shu S, Wang X, Gao L, Guo J, et al. Ligase I and ligase III mediate the DNA double-strand break ligation in alternative end-joining. Proc Natl Acad Sci U S A 2016;113:1256–60.
43. Ali R, Alabdullah M, Algethami M, Alblihy A, Miligy I, Shoqafi A, et al. Ligase 1 is a predictor of platinum resistance and its blockade is synthetically lethal in XRCC1 deficient epithelial ovarian cancers. Theranostics 2021;11:8350–61.
44. Sun L, Liu X, Song S, Feng L, Shi C, Sun Z, et al. Identification of LIG1 and LIG3 as prognostic biomarkers in breast cancer. Open Med (Wars) 2021;16: 1705–17.
45. Sun D, Urrabaz R, Nguyen M, Marty J, Stringer S, Cruz E, et al. Elevated expression of DNA ligase I in human cancers. Clin Cancer Res 2001;7:4143–8.
46. Li H, Liu Z-Y, Wu N, Chen Y-C, Cheng Q, Wang J. PARP inhibitor resistance: the underlying mechanisms and clinical implications. Mol Cancer 2020;19:107.
47. Noordermeer SM, van Attikum H. PARP inhibitor resistance: a tug-of-war in BRCA-mutated cells. Trends Cell Biol 2019;29:820–34.